CRYSTAL GROWTH & DESIGN
2007
VOL. 7, NO. 12
2594–2600

Molecular Recognition of Protonated Cytosine Ribbons by Metal–Oxalato Frameworks

Juan P. García-Terán, Oscar Castillo,* Antonio Luque,* Urko García-Couceiro, Garikoitz Beobide, and Pascual Román

Departamento de Química Inorgánica, Facultad de Ciencia y Tecnología, Universidad del País Vasco, Apartado 644, E-48080 Bilbao, Spain

Received June 27, 2007; Revised Manuscript Received September 3, 2007

ABSTRACT: A series of inorganic–organic hybrid materials, (1H,3H-cyt)$_2$[M(ox)$_2$(H$_2$O)$_2$] [M(II) = Mn (**1**), Co (**2**), Cu (**3**), Zn (**4**)] have been synthesized by the reaction of cytosine with water-soluble oxalato complexes at acidic pH. Crystallographic studies reveal that all compounds display a supramolecular three-dimensional lamellar structure knitted by wide layers of metal–oxalato complexes and planar hydrogen-bonded one-dimensional (1D) ribbonlike aggregates of protonated cytosine. The crystal building resembles that previously reported (García-Terán, J. P., et al. *Inorg. Chem.* **2007**, *46*, 3596) for the analogous 1H,9H-adeninium compound, and it is driven, in addition to electrostatic forces, by a complex network of hydrogen bonds. Nevertheless, the smaller size of the nucleobase and its different self-assembling 1D pattern lead to dissimilar molecular recognition interactions between the organic and the inorganic frameworks, which are discussed in detail.

Introduction

Over the past few decades, there has been a substantial research effort on rational design and elaboration of biomimetic systems[2] based on the interaction of nucleic acids and their building units with a wide range of both organic and inorganic frameworks.[3] The interest of these systems stems from the desire to better understand the complex interactions often present in a great diversity of molecular biorecognition processes[4] and to offer a powerful tool for the efficient synthesis of advanced functional materials with tailor-made properties and potential applications for the therapeutic medicine[5] and the material sciences.[6] Most of the studies concerning DNA/RNA nucleobases have been realized in gas phase or aqueous media,[7] but notable advances have been made in the solid-state chemistry such as (without being exhaustive): (a) the design and improvement of chemical biology tools and/or pharmaceutical agents,[8] (b) the building of high-dimensional covalent architectures containing nucleobases as bridging or terminal ligands,[9] (c) the stabilization of noncanonical tautomers through interactions with metallic ions[10] and/or hydrogen-bonding donor/acceptor species,[1,11] and (d) the development of artificial receptors for specific DNA/RNA bases recognition for their use as nucleotide sensors or for the determination of low concentrations of therapeutic agents.[12]

Following these lines of investigation, we have recently reported the elaboration and solid-state characterization of supramolecular architectures isolated from aqueous solution at physiological pH in which adenine aggregates reside between neutral one-dimensional (1D) metal–oxalato–water complexes to build sheetlike structures containing sequentially arranged organic and inorganic layers.[13] The design of non-natural receptors for biomolecules is an area of active research, examples being hosts for biologically interesting guests such as barbituric acid derivatives, creatinine, or nucleobases.[14]

Now, employing similar synthetic routes, we have succeeded in incorporating the protonated cytosine nucleobase into a metal–oxalato matrix to afford the compounds (1H,3H-cyt)$_2$[M(ox)$_2$(H$_2$O)$_2$] (M(II) = Mn (**1**), Co (**2**), Cu (**3**), and Zn [**4**]). Structural analysis of artificial systems based on cytosine and/or its protonated forms can be useful to further understand natural recognition processes involving this pyrimidine nucleobase. Protonated cytosine is present in many biochemical processes (i.e., enzymatic reactions, stabilization of triplex structures)[15] and plays a key role in a newly emerging feature of nucleic acid chemistry, namely, acid–base catalysis.[16]

Scheme 1

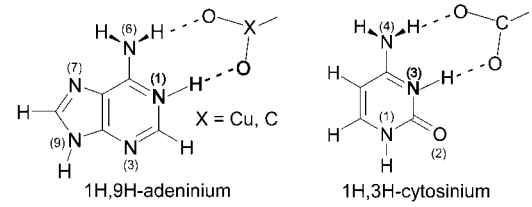

We have chosen cytosine replacing adenine as organic building block to construct analogous hybrid materials for the following reasons. First, the inorganic–organic interaction in the (1H,9H-adeninium)$_2$[Cu(ox)$_2$(H$_2$O)$_2$] compound is essentially maintained by two eight-member hydrogen-bonded $R^2_2(8)$ rings involving the N6H and N1H sites of the Watson–Crick face of the nucleobase as donors and oxalato-O atoms from O–Cu–O and O–C–O moieties as acceptors (Scheme 1). Experimental and theoretical analysis on the interaction of DNA/RNA constituents and protein building blocks[17] have shown that the last charge-assisted hydrogen bond motif exists in adeninium systems,[18] but it is also a dominant association pattern of the protonated cytosine in both biological[19] and artificial systems[20] implying the N4H/N3H edge of the nucleobase and the carboxylate groups of the amino acid (Scheme 1). Second, a perusal of the crystallographic information concerning high-dimensional aggregates of the cytosine nucleobase shows that the two previously reported homomeric self-assembling 1D patterns[21,22] for cytosinium cations are sustained by a single interaction via the exocyclic O-atom and one hydrogen atom of the N4 amino group, leaving the N4H and N3H sites as free hydrogen-bonding positions to afford forklike interactions with the carboxylate-O atoms. Third, density functional theory

* To whom correspondence should be addressed. Phone: +34 946 015 991. Fax: +34-94601-3500. E-mail: oscar.castillo@ehu.es (O.C.); antonio.luque@ehu.es.

10.1021/cg0705916 CCC: $37.00
Published on Web 11/16/2007

calculations including the presence of one $[M(ox)_2]^{2-}$ fragment in all of its possible dispositions around the cytosinium cation seem to indicate that the structural synthons found in the adeninium compound are also quite robust for assembling the cytosinium and oxalato-containing complexes.

Compounds **1**–**4** display the desired layered supramolecular structure in which homomeric cationic nucleobase ribbons are inserted between two-dimensional (2D) hydrogen-bonded sheets of metal–oxalato complexes. Nevertheless, the dissimilar arrangement of the cytosine entities along the cationic ribbon and its smaller size, with only a pyrimidinic ring, produces a different orientation of the organic and inorganic frameworks and thwarts the aforementioned forklike hydrogen-bonding interactions.

Strategies for creating reliable, reproducible inorganic–organic solid networks often depend on the combination of components that contain complementary hydrogen-bonded functionalities.[23] However, there are still many challenges to realize these tailor-made hybrid materials because the structural control is often thwarted by the delicate balance of all covalent and noncovalent forces present in the crystal building, and a slight modification of a molecular component may result in the failure to achieve the desired supramolecular interactions or even the overall three-dimensional (3D) architecture.[24]

Experimental Procedures

Syntheses. Standard literature procedures were used to prepare the starting materials $[Mn(\mu\text{-ox})(H_2O)_2]_n$, $[Co(\mu\text{-ox})(H_2O)_2]_n$, $K_2[Cu(ox)_2]\cdot 2H_2O$, and $[Zn(\mu\text{-ox})(H_2O)_2]_n$.[25]

(1H,3H-cyt)$_2$[Mn(ox)$_2$(H$_2$O)$_2$] (1). An aqueous-methanol solution (10 mL, 1/1 ratio) of cytosine (0.047 g, 0.42 mmol) was added dropwise to an aqueous solution (15 mL) of $Mn(ox)\cdot 2H_2O$ (0.025 g, 0.14 mmol) and $K_2(ox)\cdot H_2O$ (0.156 g, 0.85 mmol) with continuous stirring at 50 °C. To the resulting solution (pH 7.5), $H_2C_2O_4$ 0.1 M was added until a white precipitate of **1** appeared. Colorless X-ray quality single-crystals are obtained by slow evaporation from the mother liquor (pH 4.5). Found: C, 29.30; H, 3.25; N, 17.11; Mn, 11.06. $C_{12}H_{16}MnN_6O_{12}$ requires C, 29.34; H, 3.28; N, 17.11; Mn, 11.18%. FT-IR: ν_{max}(KBr pellet)/cm^{-1}: 3371s (ν(O–H) + ν(N$_1$–H) + ν(N$_3$–H)); 3212s, 3111s, 3065sh ν_s(NH$_2$); 3011m, 2938sh, 2910s ν(C$_5$–H); 2856w, 2711w ν(C$_6$-H); 1718vs ν(C$_5$═C$_6$); 1677s, 1645vs ν_{as}(O–C–O); 1585s δ(NH$_2$); 1543s, 1486w ν(N$_3$–C$_4$); 1435s δ(N$_1$–H); 1340m δ(C$_6$–H); 1300s ν_s(O–C–O); 1227s, ν(C$_2$–N$_3$); 1108w δ(C$_5$–H); 1089w δ_{ro}(NH$_2$); 1000m δ(R1); 969m, 942m γ(C$_6$–H); 908w, 892w ν(N$_3$–C$_4$); 833w ν(C$_2$═O); 789s (ν(C$_2$═O) + δ(O–C–O)); 762m, 711w (γ(C$_2$═O) + γ(C$_5$–H)); 669sh, 640w, 607w (γ(C$_5$–H) + γ(N$_1$–H)); 584s δ(R2); 541w (δ(R3) + τ(NH$_2$)); 522s, 500m, 473m, 436m ν(M–O).

(1H,3H-cyt)$_2$[Co(ox)$_2$(H$_2$O)$_2$] (2). The synthesis for compound **2** is similar to that described for **1** but replacing $Mn(ox)\cdot 2H_2O$ by $Co(ox)\cdot 2H_2O$ (0.026 g, 0.14 mmol). Again, acidification with $H_2C_2O_4$ 0.1 M leads to **2** as a pinkish precipitate. Pink crystals suitable for X-ray determination were obtained from the mother liquid (pH 5.6) after few days. Found: C, 28.96; H, 3.18; N, 17.00; Co, 11.78. $C_{12}H_{16}CoN_6O_{12}$ requires C, 29.10; H, 3.26; N, 16.97; Co, 11.90%. FT-IR: ν_{max}(KBr pellet)/cm^{-1}: 3368s (ν(O–H) + ν (N$_1$–H) + ν (N$_3$–H)); 3217s, 3116s, 3073sh ν $_s$(NH$_2$); 3007m, 2944sh, 2909s ν (C$_5$–H); 2859w, 2711w ν (C$_6$–H); 1717vs ν (C$_5$═C$_6$); 1680s, 1645vs ν_{as}(O–C–O); 1593s δ(NH$_2$); 1545s, 1485w ν (N$_3$–C$_4$); 1436s δ(N$_1$–H); 1345m δ(C$_6$–H); 1304s ν_s(O–C–O); 1228s ν (C$_2$–N$_3$); 1111w δ(C$_5$–H); 1089w δ_{ro}(NH$_2$); 1002m δ(R1); 970m, 933m γ(C$_6$–H); 894w ν (N$_3$–C$_4$); 833w ν(C$_2$═O); 792s (ν (C$_2$═O) + δ(O–C–O)); 764m, 722w (γ(C$_2$═O) + γ(C$_5$–H)); 670w 623w (γ(C$_5$–H) + γ(N$_1$–H)); 586s δ(R2); 541w (δ(R3) + τ(NH$_2$)); 525s, 475m, 439m ν (M-O).

(1H,3H-cyt)$_2$[Cu(ox)$_2$(H$_2$O)$_2$] (3). An aqueous-methanol solution (10 mL, 1/1 ratio) of cytosine (0.047 g, 0.42 mmol) was added dropwise to an aqueous–methanol solution (15 mL, 2/1 ratio) of $K_2[Cu(ox)_2]\cdot 2H_2O$ (0.050 g, 0.14 mmol) and $K_2(ox)\cdot H_2O$ (0.026 g, 0.14 mmol) with continuous stirring. Light-blue crystals of compound **3** were obtained by the slow diffusion of this mixture into an aqueous solution of 0.1 M HNO_3. Crystal growth was observed after three weeks. Found: C, 28.64; H, 3.10; N, 16.80; Cu, 12.58. $C_{12}H_{16}CuN_6O_{12}$ requires C, 28.84; H, 3.23; N, 16.81; Cu, 12.71%. FT-IR: ν_{max}(KBr pellet)/cm^{-1}: 3410sh, 3358s (ν(O–H) + ν(N$_1$–H) + ν(N$_3$–H)); 3154sh, 3114s, 3069sh ν_s(NH$_2$); 3006s, 2941sh, 2917s ν(C$_5$–H); 2855w, 2742m, 2705m ν(C$_6$–H); 1720vs ν(C$_5$═C$_6$); 1685s, 1662vs ν_{as}(O–C–O); 1607s δ(NH$_2$); 1540s, 1477w ν(N$_3$–C$_4$); 1423s δ(N$_1$–H), 1342m δ(C$_6$–H); 1293s ν_s(O–C–O); 1225s ν(C$_2$–N$_3$); 1131w, 1115w δ(C$_5$–H); 1091w δ_{ro}(NH$_2$); 1003m δ(R1); 972m, 944w γ(C$_6$–H); 918w, 893w ν(N$_3$–C$_4$); 829m ν(C$_2$═O); 797s, (ν(C$_2$═O) + δ(O–C–O)); 763w, 744w (γ(C$_2$═O) + γ(C$_5$–H)); 696m, 661s, 634sh (γ(C$_5$–H) + γ(N$_1$–H)); 583s δ(R2); 542m (δ(R3) + τ(NH$_2$)); 513s, 480m, 439m ν(M–O).

(1H,3H-cyt)$_2$[Zn(ox)$_2$(H$_2$O)$_2$] (4). The synthesis for compound **4** is similar to that described for **1** but replacing $Mn(ox)\cdot 2H_2O$ by $Zn(ox)\cdot 2H_2O$ (0.027 g, 0.14 mmol). Likewise, after acidification with $H_2C_2O_4$ 0.1M, a white powder of **4** precipitates. Colorless X-ray quality single-crystals are obtained by evaporation from the mother liquid (pH 4.8). Found: C, 28.62; H, 3.11; N, 16.85; Zn, 12.90. $C_{12}H_{16}N_6O_{12}Zn$ requires C, 28.73; H, 3.21; N, 16.75; Zn, 13.03%. FT-IR: ν_{max}(KBr pellet)/cm^{-1}: 3368s (ν(O–H) + ν(N$_1$–H) + ν(N$_3$–H)); 3213s, 3116s, 3073sh ν_s(NH$_2$); 3007m, 2944sh, 2913s ν(C$_5$–H); 2859w, 2711w ν(C$_6$–H); 1717vs ν(C$_5$═C$_6$); 1679s, 1647vs ν_{as}(O–C–O); 1597s δ(NH$_2$); 1543s, 1482w ν(N$_3$–C$_4$); 1436s δ(N$_1$–H); 1348m δ(C$_6$–H); 1303s ν_s(O–C–O); 1226s ν(C$_2$–N$_3$); 1108w δ(C$_5$–H); 1092w δ_{ro}(NH$_2$); 1000m δ(R1); 970m, 932m γ(C$_6$–H); 886w ν(N$_3$–C$_4$); 833w ν(C$_2$═O); 793s (ν(C$_2$═O) + δ(O–C–O)); 762m, 711w (γ(C$_2$═O) + γ(C$_5$–H)); 667w, 650w (γ(C$_5$–H) + γ(N$_1$–H)); 587s δ(R2); 544w (δ(R3) + τ(NH$_2$)); 524s, 478m, 440m ν(M–O).

It is necessary to note that the yields of the above-described synthetic methods are usually below 30% and that they have been employed to obtain suitable specimens for the X-ray single-crystal diffraction analysis. Nevertheless, pure powder samples of all the compounds can also be obtained in almost quantitative yield by slow acidification at pH below 4.0. The purity and homogeneity of these polycrystalline samples were checked by IR spectroscopy, elemental analysis, and X-ray powder diffraction methods.

Physical Measurements. Elemental analyses (C, H, N) were performed on a Perkin-Elmer 2400 microanalytical analyzer. Metal content was determined by absorption spectrometry. The IR spectra (KBr pellets) were recorded on a FTIR Mattson 1000 spectrometer in the 4000–400 cm^{-1} spectral region. Thermal analyses (TG/DTA) were performed on a TA Instruments SDT 2960 thermal analyzer in a synthetic air atmosphere (79% N_2/21% O_2) with a heating rate of 5 °C min^{-1}.

X-ray Structural Studies. Diffraction data were collected at 293(2) K on an Oxford Xcalibur diffractometer with graphite-monochromated Mo-K_α radiation (λ = 0.71073 Å). The data reduction was done with the CrysAlis RED program.[26] Structures were solved by direct methods using the SIR 92 program[27] and refined by full-matrix least-squares on F^2 including all reflections (SHELXL97).[28] All calculations were performed using the WinGX crystallographic software package.[29] Crystal parameters and details of the final refinements of compounds **1**–**4** are summarized in Table 1.

Computational Details. All the quantum mechanical calculations of geometry optimizations have been carried out in gas phase using the density functional theory with Becke's three-parameter exchange functional[30] along with the Lee–Yang–Parr nonlocal correlation functional (B3LYP).[31] The standard 6–31G(d) basis set was used as implemented in the Gaussian03 program.[32] It is well known that although the B3LYP functional method might not be suitable for the consistent study of the whole range of the DNA base interactions due to its insufficiency in describing the dispersion interactions, it predicts reliable interaction energies for hydrogen bonded systems.[33]The interaction energies were corrected for the basis set superposition error (BSSE) using the standard Boys–Bernardi counterpoise correction scheme.[34]

Results and Discussion

Structural Description. X-ray diffraction analysis of compounds **1**–**4** shows that they are isomorphous and crystallize in the monoclinic space group $P2_1/c$ (No. 14). Their crystal structures consist of centrosymmetric *trans*-$[M(ox)_2(H_2O)_2]^{2-}$ anions and cytosinium cations (with protons at the N1 and N3 sites) linked together by electrostatic interactions and an intricate network of hydrogen bonds. A perspective view of the structural

Table 1. Single-Crystal Data and Structure Refinement Details for Compounds 1–4

	1	2	3	4
formula	$C_{12}H_{16}MnN_6O_{12}$	$C_{12}H_{16}CoN_6O_{12}$	$C_{12}H_{16}CuN_6O_{12}$	$C_{12}H_{16}N_6O_{12}Zn$
formula weight	491.25	495.24	499.85	501.68
crystal size (mm^3)	0.12 × 0.08 × 0.06	0.12 × 0.07 × 0.03	0.18 × 0.10 × 0.06	0.07 × 0.04 × 0.02
crystal system	monoclinic	monoclinic	monoclinic	monoclinic
space group	$P2_1/c$	$P2_1/c$	$P2_1/c$	$P2_1/c$
a (Å)	9.478(3)	9.492(2)	9.550(1)	9.528(2)
b (Å)	7.021(2)	6.948(2)	6.967(1)	6.962(1)
c (Å)	13.893(4)	13.499(2)	13.767(3)	13.565(2)
β (deg)	107.49(4)	107.14(2)	107.70(2)	107.18(2)
V ($Å^3$)	881.8(5)	850.7(3)	872.6(3)	859.7(3)
Z	2	2	2	2
ρ_{calc} ($g\cdot cm^{-3}$)	1.850	1.933	1.902	1.938
ρ_{obs} ($g\cdot cm^{-3}$)	1.84(1)	1.92(1)	1.89(1)	1.93(1)
μ(mm^{-1})	0.840	1.097	1.337	1.516
F(000)	502	506	510	512
reflns collected	8603	7243	4994	5010
reflns unique	2555	2056	2552	2548
R_{int}	0.0573	0.0912	0.0570	0.0802
R_1 [$I \geq 2\sigma(I)$]	0.0473	0.0348	0.0450	0.0426
wR_2 [$I \geq 2\sigma(I)$]	0.1222	0.1388	0.1005	0.1156
R_1 (all data)	0.0881	0.1026	0.0764	0.1134
wR_2 (all data)	0.1268	0.1443	0.1101	0.1243

units of compound **2**, with the atomic numbering scheme, is given in Figure 1. Selected bond lengths and angles for the coordination polyhedron are gathered in Table 2, whereas Table 3 lists the structural parameters of the noncovalent interactions between the building units.

The coordination polyhedron of the metal atom, which sits on a crystallographic inversion center, is a distorted octahedron with an equatorial plane formed by four oxygen atoms from two bidentate oxalato ligands and with water molecules in the axial sites to give a $O_4(O_w)_2$ donor set. The equatorial chelated rings are nearly planar, and the M–Ow axial bonds are longer than the equatorial bonds in good agreement with the axial elongation found in other *trans*-diaquabis(oxalato-O,O′)-metalate(II) complexes.[1,35] This effect is more marked for compound **3** owing to the expected tetragonal Jahn–Teller elongation of the copper(II) octahedron.[36]

Adjacent anionic complexes are joined by means of short hydrogen bonds O1w–H···O_{ox} giving rise to sheets that spread out along the crystallographic *bc* plane (Figure 2a). The anionic complexes are oriented in two different directions which form between them an angle of 63° to give a layer with a thickness

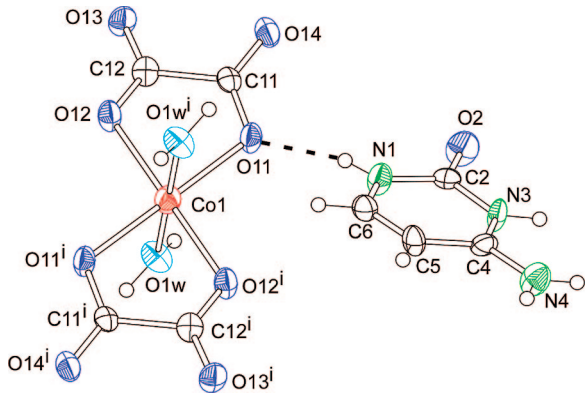

Figure 1. Perspective drawing of structural units of compound **2**. Displacements ellipsoids are drawn at 50% probability. Symmetry code: $-x$, $2-y$, $2-z$.

Table 2. Selected Bond Lengths (Å) and Bond Angles (deg) for Compounds 1–4[a]

	1	2	3	4
M–O(11)	2.166(2)	2.079(2)	1.968(2)	2.073(3)
M–O(12)	2.137(2)	2.040(2)	1.948(2)	2.039(3)
M–O(1w)	2.237(2)	2.122(2)	2.436(2)	2.195(3)
O(11)–M–O(12)	77.68(8)	80.33(7)	84.37(8)	81.41(11)
O(11)–M–O(12)^i	102.32(8)	99.67(7)	95.63(8)	98.59(11)
O(11)–M–O(1w)	86.79(8)	88.21(7)	88.22(8)	87.88(11)
O(11)–M–O(1w)^i	93.21(8)	91.79(7)	91.78(8)	92.12(11)
O(12)–M–O(1w)	88.39(8)	89.14(7)	88.56(8)	88.97(11)
O(12)–M–O(1w)^i	91.61(8)	90.86(7)	91.44(8)	91.03(11)

[a] Symmetry codes: (i) $-x$, $2-y$, $2-z$.

Table 3. Selected Structural Parameters (Å, deg) for Compounds 1–4[a]

D–H···A[b]	H···A	D···A	D–H···A
	1		
O(1w)–H(11w)···O(13)^i	1.88	2.682(3)	154
O(1w)–H(12w)···O(14)^{ii}	1.90	2.778(3)	166
N(1)–H(1)···O(11)^{iii}	1.98	2.820(3)	164
N(3)–H(3)···O(13)^{iv}	1.88	2.742(3)	175
N(4)–H(4A)···O(1w)^v	2.21	3.036(4)	162
N(4)–H(4B)···O(2)^i	2.22	3.017(3)	155
	2		
O(1w)–H(11w)···O(13)^i	1.79	2.669(3)	166
O(1w)–H(12w)···O(14)^{ii}	1.92	2.769(2)	167
N(1)–H(1)···O(11)^{iii}	1.95	2.786(3)	164
N(3)–H(3)···O(13)^{iv}	1.89	2.749(3)	176
N(4)–H(4A)···O(1w)^v	2.18	3.017(3)	163
N(4)–H(4B)···O(2)^i	2.18	2.977(3)	155
	3		
O(1w)–H(11w)···O(13)^i	1.90	2.728(3)	166
O(1w)–H(12w)···O(14)^{ii}	1.98	2.828(4)	173
N(1)–H(1)···O(11)^{iii}	1.98	2.808(3)	160
N(3)–H(3)···O(13)^{iv}	1.87	2.733(3)	178
N(4)–H(4A)···O(1w)^v	2.12	2.945(4)	161
N(4)–H(4B)···O(2)^i	2.25	3.034(3)	152
	4		
O(1w)–H(11w)···O(13)^i	1.98	2.696(4)	148
O(1w)–H(12w)···O(14)^{ii}	1.91	2.767(4)	150
N(1)–H(1)···O(11)^{iii}	1.96	2.797(4)	163
N(3)–H(3)···O(13)^{iv}	1.88	2.744(5)	177
N(4)-H(4A)···O(1w)^v	2.19	3.015(5)	161
N(4)–H(4B)···O(2)^i	2.20	2.990(4)	153

[a] Symmetry codes: (i) x, $1+y$, z; (ii) $-x$, $1/2+y$, $3/2-z$; (iii) $-x$, $-1/2+y$, $3/2-z$; (iv) $1-x$, $1-y$, $2-z$; (v) $1-x$; $2-y$; $2-z$. [b] D: donor; A: acceptor.

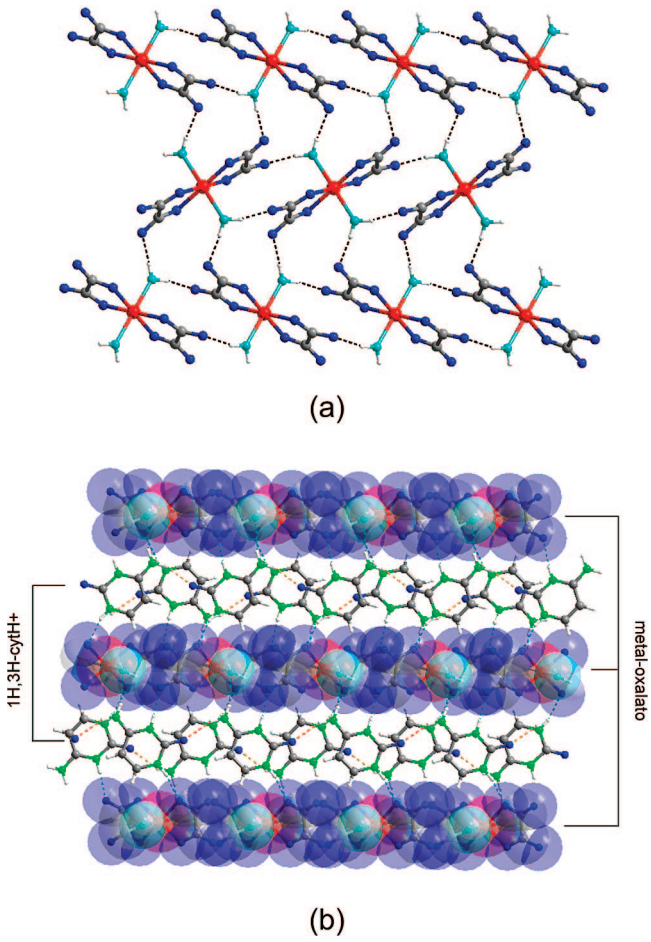

Figure 2. (a) Ball and stick representation of the inorganic sheet. (b) Crystal packing of compounds **1**–**4** showing the alternating inorganic–organic layers. Hydrogen bonds are shown as dashed lines.

of ca. 6.5 Å. The space between the anionic layers is occupied by perpendicularly arranged organic cations that cross-link the nearest-neighbor layers by means of N–H···O hydrogen bonds to afford the predicted supramolecular inorganic–organic hybrid 3D architecture (Figure 2b). Furthermore, cytosinium cations undergo association along the *b* axis through intermolecular hydrogen bonding to form ribbon-like 1D supramolecular aggregates in which the nucleobases are coplanar.

Nucleobases, either protonated or nonprotonated, have multi-hydrogen-bonding sites of special geometry arrangement in such a way that they have a great tendency to form extended aggregates. Autoassembly into high-dimensional nanoscale arrangements (ribbons, monolayers, or even bilayers) stabilized by hydrogen bonds between molecules is common, especially when the neutral nucleobases are deposited onto various insulating or metal surfaces.[37] Compounds isolated from solution show a strong competition for all the important hydrogen-bonding donor and acceptor sites,[38] and as a consequence high-order aggregates are not usual. The crystal structures of nearly 80 compounds containing the canonical 1H-tautomer of cytosine or its protonated forms have been retrieved from the Cambridge Structural database (CSD, May 2007 release),[39] and five different 1D nucleobase patterns have been found (Figure 3). Neutral cytosine is usually coordinated to metallic centers and 1D homonucleobase aggregates (A) are only observed in the crystal structure of cytosine[40] and cytosine monohydrate[41] in which nucleobases are linked by means of N1–H···N3 and N4–H···O=C hydrogen bonds. Nucleobase protonation seems

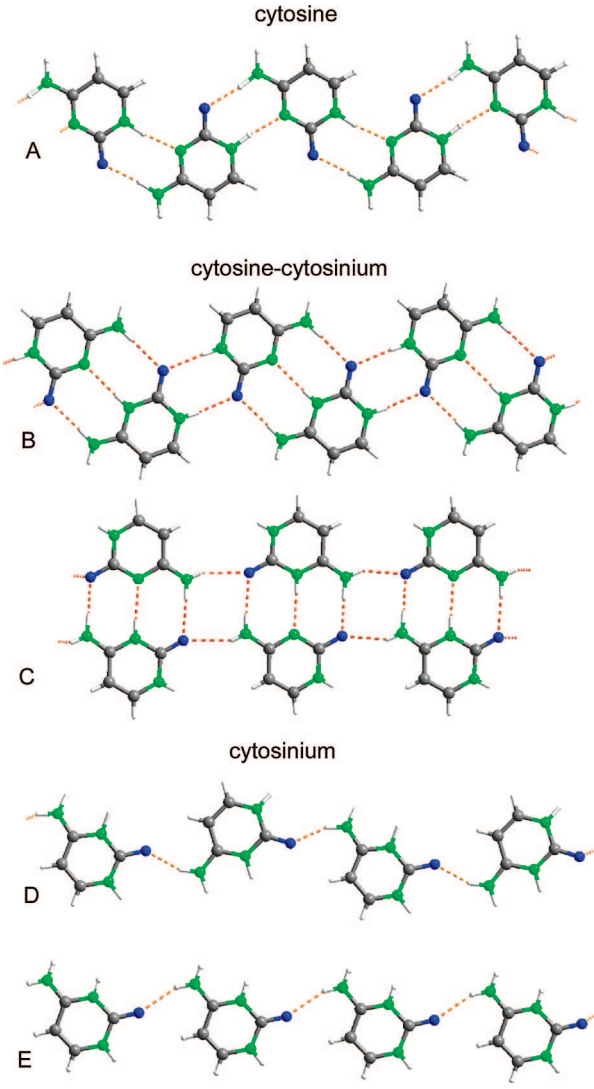

Figure 3. Self-assembled 1D aggregates involving cytosine and/or 1H,3H-cytosinium.

to increase the possibility of self-aggregation and the number of available crystal structures with cationic 1D ribbons is greater. Mixed cytosine–cytosinium systems contain base pairs connected by three hydrogen bonds, two of which involve the N4 hydrogen bond donors and O2 hydrogen bond acceptors, while the third is formed between the protonated N3 atom of one base and the unprotonated N3 site of the other base, thus resembling a pseudo-Watson–Crick pattern. Furthermore, the adjacent $CytHCyt^+$ pairs are held together by double N1H···O=C[42,43] or N4H···O=C[18d,43] hydrogen bonds leading to two different types of 1D supramolecular polymeric ribbons (B, C) with alternating neutral and protonated cytosine entities. Concerning the 1H,3H-cytosinium cation, two 1D self-assembling patterns (D, E) have been reported, and both are sustained by means of a single N4–H···O2 hydrogen-bonding interaction. The organic ribbon in compounds **1**–**4** exhibits an E type self-assembled pattern with donor···acceptor distances [from 2.977(3) to 3.034(3) Å] similar to those found for previously reported cytosinium chains (ranging from 2.759 to 3.031 Å).[21,22] The number of free hydrogen-bond sites (including the N4 and N3 sites) in the D and E arrangements is greater than that provided by other chains, and therefore, the demanding conditions for more extensive secondary hydrogen-bonding interactions with

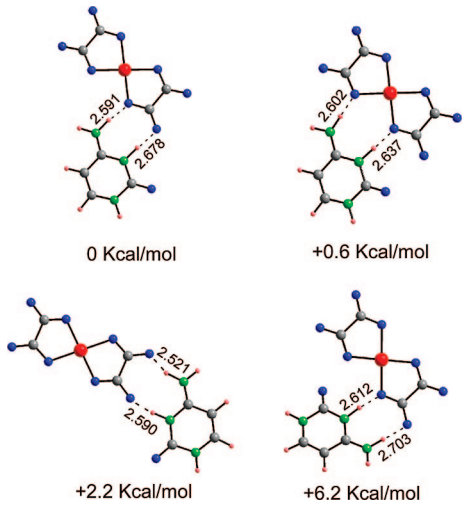

Figure 4. Most plausible interaction of the cytosinium N4H/N3H edge with a metal–oxalato framework.

the carboxylate-O atoms of adjacent inorganic complexes are better fulfilled by these cytosinium–cytosinium self-assembling patterns.

Interactions between nucleobases and carboxylate groups have been extensively studied both in solution and by X-ray crystallographic methods to understand the elementary stereochemical patterns in protein–nucleic acid recognition mechanisms involving amino acid carboxylic groups.[17] One of the most frequent interactions for 1H,3H-cytosinium and 1H,9H-adeninium systems is a charge-assisted planar $R_2^2(8)$ hydrogen bond connecting the HN_{exo}–C–NH fragment of the protonated nucleobase (N4H/N3H edge of cytosine, Watson–Crick N6H/N1H edge of adenine) as donor sites and the O-atoms of one anionic carboxylate entity as acceptor group (Scheme 1). The efficiency of the molecular recognition pattern is so high that in some cases the N1/N3 position of a neutral nucleobase has become protonated by the proton transfer from the carboxylic group–upon a molecular recognition process.[44] The biological and chemical importance of this forklike hydrogen-bonding interaction for the cytosine nucleobase is reflected by its participation in the active sites of several enzymes that catalyze chemical transformations of cytidine such as deamination to uridine[45] or hydroxymethylation,[19] and by the crystallographic information retrieved from 22 X-ray structures compiled in the CSD containing cytosinium entities and anionic carboxylate moieties. Fourteen of them exhibit this structural synthon, and the coordination of the nucleobase or its dimerization to form the highly stable three hydrogen-bonded $CytHCyt^+$ base pair[46] precludes the interaction in the remaining crystal buildings. The organic–inorganic assembling of the above-cited $(1H,9H\text{-adeninium})_2[Cu(ox)_2(H_2O)_2]$ compound is essentially driven by this charge-assisted structural motif together with other similar $R_2^2(8)$ rings involving O–Cu–O fragments, which is 10.32 kcal/mol more stable than the first one.[1]

To get a deeper insight into the interaction of the 1H,3H-cytosinium cation with a metal–oxalato fragment, we have optimized the most plausible arrangements between the organic cation and a $[Cu(ox)_2]^{2-}$ complex anion (Figure 4). The results indicate that the interaction implying the N4H/N3H donor sites with one O–C–O group is the most favorable with an energy difference of 0.56 kcal/mol with respect to that involving the O–Cu–O fragment. Furthermore, both optimized structures show relatively strong hydrogen-bonding interactions with values of the geometric parameters within the lower limit of the range found for forklike structural motifs (N4···O: 2.639–2.996 Å; N3···O: 2.565–2.868 Å) in cytosine–carboxylato crystal structures retrieved from the CSD database.

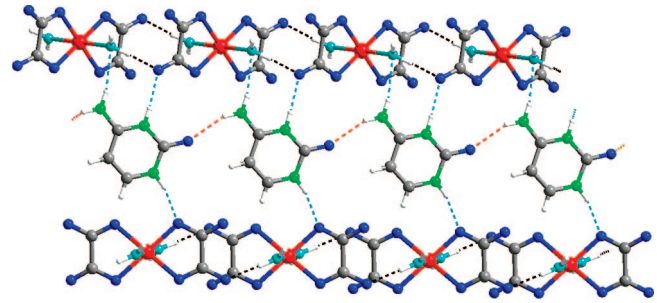

Figure 5. Interaction between the organic and inorganic building blocks in the crystal structures of compounds **1**–**4**.

In the light of the above considerations, it occurred to us that the pyrimidine nucleobase could be, a priori, exploited as an organic motif for the crystal engineering of self-assembled hybrid structures resembling that previously reported for the 1H,9H-adeninium cation. This assumption was confirmed by the overall sheetlike structure of compounds **1**–**4**, but the projected forklike interactions are absent owing to the distinctive features of the self-assembling pattern of the nucleobase ribbons.

In the case of the 1H,9H-adeninium compound, the protonated Watson–Crick face of the cations (H6–N6–C6–N1–H) are alternately placed in both sides of the 1D aggregate with a distance of 11.649 Å between two consecutive ones, which allows the coplanar stacking of the $[Cu(ox)_2]$ fragments close to both sides of the nucleobase ribbon.[1] The length of a $[M(ox)_2]$ fragment is around 10.5 Å, and monomer–monomer distances ranging from 11 to 12.0 Å have been previously reported for crystal structures with a coplanar stacking of diaquabis(oxalato)metallate anions.[47] The coplanar organic–inorganic disposition makes easier the establishment of forklike interactions with both sides of the ribbon, one of them linked to the O_{ox}–Cu–O_{ox} fragments, while the opposite one attached to O–C–O carboxylato groups of the adjacent inorganic sheet.

At first sight, a type D ribbon pattern of cytosinium would then be adequate to provide a coplanar stacking of the structural entities because the N4H/N3H edges are also alternately placed along the 1D aggregate with a distance of 13.5 Å between two consecutives ones.[22] Nevertheless, compounds **1**–**4** show a 1D aggregate of type E in which the N4H/N3 faces of the cytosinium cations are located on the same side of the ribbon with a distance of ca. 7.0 Å (coincident with the crystallographic *b*-parameter). This value matches very well with those found for other chains of this type (ranging from 6.870 to 7.110 Å),[21] and it is not long enough to allow the coplanar stacking of $[M(ox)_2]$ fragments along the nucleobase ribbon, so that the nearest anionic complexes are twisted to avoid steric hindrances, and dihedral angles between the planar ribbons and the $[M(ox)_2]$ fragments of around 30° are observed, precluding the anticipated forklike hydrogen-bonding interactions with the O–C–O and O–M–O units. N4–H and N3–H sites of the cytosinium cation act as hydrogen-bonding donors toward oxygen atoms from one oxalato ligand and one water molecule of a neighboring anionic complex belonging to the same inorganic sheet. The oxygen atoms are hydrogen bonded one to each other to complete a cyclic $R_3^2(8)$ ring. The adhesive-tape role of the organic ribbons is completed by a N–H···O_{ox} interaction between the N1–H group of the cytosinium cation and one oxalato oxygen atom from the adjacent anionic sheet (Figure 5).

DFT calculations have been performed to check the stability of the hydrogen-bonding environment around the cytosinium moiety. Hydrogen-bond lengths in the optimized structure show trends similar to those found in compounds **1–4**, but absolute values are shorter in the calculated structure with N4···O1w and N3···O13 distances of 2.834 and 2.598 Å, respectively. The observed hydrogen-bonded $R_3^2(8)$ interaction has not been previously reported in nucleobase artificial systems, but it resembles that found in the end cap of the binding pocket of the vaccinia VP39 virus protein[48] used to discriminate alkylated from nonalkylated nucleobases, and it has been also found in a handful of crystal structures involving the melaminium cation and carboxylate groups.[49]

Inorganic–organic supramolecular recognition patterns of cytosinium and adeninium compounds are both quite effective since the compounds show a close crystal packing with high values of the crystal density (1.90 and 1.92 g cm^{-3} for the copper(II) complexes of cytosinium and adeninium, respectively). They do not exhibit the presence of crystallization–water molecules in contrast to what usually occurs in the crystal building of compounds with discrete *trans*-$[M(ox)_2(H_2O)_2]$ entities in which solvation molecules are filling the channels or holes generated by the arrangement of the structural units.[35b,50] The robustness of the overall supramolecular 3D architecture is confirmed by the high thermal stability of the compounds for which thermal degradations in synthetic air take place above 170 °C without clear discrimination of the lost weight attributable to the coordinated water molecules and the pyrolysis of the organic molecules.

Conclusion

In this work, we have clearly demonstrated that metal–oxalato systems can act as receptors of highly ordered cytosine architectures, as previously thought on the basis of the experimental data provided by our previous research about oxalato–adenine systems. As the adeninium compounds, the supramolecular 3D assembling of the structural units is again driven, together with the electrostatic forces, by a synergy of three types of molecular recognition: (a) between nucleobase cations which leads to the organic ribbon form, (b) between ribbons of nucleobases and anionic complexes, and (c) between complex anions within the inorganic layers to complete the very effective set of interactions and to build the closely packed structures. Nonetheless, the distinctive self-assembling 1D pattern of the 1H,3H-cytosinium and 1H,9H-adeninium cations results in dissimilar hydrogen-bonding motifs between the nucleobases and the metal–oxalato frameworks, and as a consequence, produces relevant changes in the structural parameters of these organic–inorganic hybrid materials. This study can contribute to a further understanding of the molecular recognition processes between nucleobases and artificial receptors and is therefore relevant to biological inorganic chemistry.

Acknowledgment. Financial support from the Ministerio de Educación y Ciencia (MAT2005-03047) and the Universidad del País Vasco/Euskal Herriko Unibertsitatea (GIU06/72) is gratefully acknowledged. J.P.G-T. thanks Eusko Jaurlaritza/Gobierno Vasco for a predoctoral fellowship. The SGI/IZO-SGIker UPV/EHU (supported by the National Program for the Promotion of Human Resources within the National Plan of Scientific Research, Development and Innovation, Fondo Social Europeo and MCyT) is gratefully acknowledged for generous allocation of computational resources.

Supporting Information Available: X-ray crystallographic files in CIF format for crystals **1–4**. This material is available free of charge via the Internet at http://pubs.acs.org.

References

(1) García-Terán, J. P.; Castillo, O.; Luque, A.; García-Couceiro, U.; Beobide, G.; Román, P. *Inorg. Chem.* **2007**, *46*, 3596.
(2) Derose, V. J.; Burns, S.; Kim, N. K.; Vogt, M. In *Comprehensive Coordination Chemistry II*; McCleverty, J. A., Meyer, T. J., Eds.; Elsevier: University of Bern, Switzerland, 2004; Vol. 8, pp 787–813.
(3) (a) Richards, A. D.; Rodger, A. *Chem. Soc. Rev.* **2007**, *36*, 471. (b) Chifotides, H. T.; Dunbar, K. R. *Acc. Chem. Res.* **2005**, *38*, 146. (c) Navarro, J. A. R.; Lippert, B. *Coord. Chem. Rev.* **2001**, *222*, 219.
(4) Hannon, M. J. *Chem. Soc. Rev.* **2007**, *36*, 280.
(5) Natile, G.; Marzilli, L. G. *Coord. Chem. Rev.* **2006**, *250*, 1315.
(6) (a) Santoso, S. S.; Zhang, S. In *Encyclopedia of Nanoscience and Nanotechnology*; Nalwa, H. S. Ed.; American Scientific Publishers: Valencia, CA, 2004; Vol. 9, pp 459–471. (b) Simmel, F. C.; Yurke, B. In *Encyclopedia of Nanoscience and Nanotechnology*; Nalwa, H. S. Ed.; American Scientific Publishers: Valencia, CA, 2004; Vol. 2, pp. 495–504.
(7) (a) Fonseca-Guerra, C.; Bickelhaupt, F. M.; Saha, S.; Wang, F. *J. Phys. Chem. A* **2006**, *110*, 4012. (b) Hanus, M.; Kabelac, M.; Rejnek, J.; Ryjacek, F.; Hobza, P. *J. Phys. Chem. B* **2004**, *108*, 2087.
(8) Legraverend, M.; Grierson, D. S. *Bioorg. Med. Chem.* **2006**, *14*, 3987.
(9) (a) González-Pérez, J. M.; Alarcón-Payer, C.; Castiñeiras, A.; Pivetta, T.; Lezama, L.; Choquesillo-Lazarte, D.; Crisponi, G.; Niclós-Gutiérrez, J. *Inorg. Chem.* **2006**, *45*, 877. (b) Das, S.; Madhavaiah, C.; Verma, S.; Bharadwaj, P. K. *Inorg. Chim. Acta* **2005**, *358*, 3236. (c) Olea, D.; Alexandre, S. S.; Amo-Ochoa, P.; Guijarro, A.; de Jesús, F.; Soler, J. M.; de Pablo, P. J.; Zamora, F.; Gomez-Herrero, J. *Adv. Mater.* **2005**, *17*, 1761. (d) García-Terán, J. P.; Castillo, O.; Luque, A.; García-Couceiro, U.; Román, P.; Lezama, L. *Inorg. Chem.* **2004**, *43*, 4549.
(10) (a) Rojas-González, P. X.; Castiñeiras, A.; González-Pérez, J. M.; Choquesillo-Lazarte, D.; Niclós-Gutiérrez, J. *Inorg. Chem.* **2002**, *41*, 6190. (b) Zamora, F.; Kunsman, M.; Sabat, M.; Lippert, B. *Inorg. Chem.* **1997**, *36*, 1583.
(11) García-Terán, J. P.; Castillo, O.; Luque, A.; García-Couceiro, U.; Beobide, G.; Román, P. *Dalton Trans.* **2006**, *902*.
(12) (a) Lee, S. C. ; Ruegsegger, M. A.; Ferrari, M. In *Encyclopedia of Nanoscience and Nanotechnology*; Nalwa, H. S., Ed.; American Scientific Publisers: Valencia, CA, 2004; Vol. 1, pp 309–327. (b) Mancin, F.; Chin, J. *J. Am. Chem. Soc.* **2002**, *124*, 10946.
(13) García-Terán, J. P.; Castillo, O.; Luque, A.; García-Couceiro, U.; Román, P.; Lloret, F. *Inorg. Chem.* **2004**, *43*, 5761.
(14) (a) Alkorta, I.; Elguero, J.; Goswami, S.; Mukherjee, R. *J. Chem. Soc., Perkin Trans. 2* **2002**, 894. (b) Luth, M. S.; Freisinger, E.; Lippert, B. *Chem. Eur. J.* **2001**, *7*, 2104.
(15) (a) Boulard, Y.; Cognet, J. A.; Fazakerly, G. V. *J. Mol. Biol.* **1997**, *268*, 331. (b) Vlieghe, D.; van Meervalt, L.; Dautant, A.; Gallois, B.; Precigoux, C.; Kennard, O. *Science* **1996**, *273*, 1702. (c) Wu, M.; McDowell, J. A.; Turner, D. H. *Biochemistry* **1995**, *34*, 3204. (d) Gehring, K.; Leroy, J. L.; Gueron, M. *Nature* **1993**, *363*, 561.
(16) Lippert, B. In *Progress in Inorganic Chemistry*; Karlin, K. D., Ed.; John Wiley and Sons: New York, 2005; Vol. 54, pp 385–447.
(17) Cheng, A. C.; Frankel, A. D. *J. Am. Chem. Soc.* **2004**, *126*, 434.
(18) (a) Johansson, T.; Oswald, C.; Pedersen, A.; Törnroth, S.; Okvist, M.; Karlsson, G.; Rydström, J.; Krengel, U. *J. Mol. Biol.* **2005**, *352*, 299. (b) Smith, G.; Wermuth, U. D.; Healy, P. C. *Acta Crystallogr.* **2004**, *E60*, o1573. (c) Serrano-Pardial, E.; Choquesillo-Lazarte, D.; Bugella-Altamirano, E.; Castiñeiras, A.; Carballo, R.; Niclós-Gutiérrez, J. *Polyhedron* **2002**, *21*, 1451. (d) Salam, M. A.; Aoki, K. *Inorg. Chim. Acta* **2000**, *311*, 15. (e) Takusagawa, F.; Bergman, H. M.; Dabrow, M.; Robins, R. K. *Acta Crystallogr.* **1985**, *C41*, 400.
(19) (a) Yao, L.; Sklenak, S.; Yan, H.; Cukier, R. I. *J. Phys. Chem. B* **2005**, *109*, 7500. (b) Song, H. K.; Sohn, S. H.; Suh, S. W. *EMBO J.* **1999**, *18*, 1104.
(20) (a) Bouchouit, K.; Benali-Cherif, N.; Dahaoui, S.; Beneif, E. E.; Lecomte, C. *Acta Crystallogr.* **2005**, *E61*, o2755. (b) Doi, M.; Nakamoto, Y.; Asano, A. *Acta Crystallogr.* **2005**, *C61*, o577. (c) Smith, G.; Wermuth, U. D.; Healy, P. C. *Acta Crystallogr.* **2005**, *E61*, o746. (d) Davies, R. G.; Gibson, V. C.; Hursthouse, M. B.; Light, M. E.; Marshall, E. L.; North, M.; Robson, D. A.; Thompson, I.; White, A. J. P.; Williams, D. J.; Williams, P. J. *J. Chem. Soc., Perkin Trans. 1* **2001**, 3365. (e) Balsubramanian, T.; Muthiah, P. T.; Robinson, W. T. *Bull. Chem. Soc. Jpn.* **1996**, *69*, 2919.

(21) (a) Bouacida, S.; Merazig, A.; Beghidja, A.; Beghidja, C. *Acta Crystallogr.* **2005**, *E61*, m2072. (b) Gorbitz, C. H.; Sagstuen, E. *Acta Crystallogr.* **2004**, *E60*, o1945. (c) Jaworski, S.; Schollborn, H.; Eisenmann, P.; Thewalt, U.; Lippert, B. *Inorg. Chim. Acta* **1988**, *153*, 31. (d) Bourne, P. E.; Taylor, M. R. *Acta Crystallogr.* **1983**, *C39*, 430. (e) Ogawa, K.; Nishitani, K.; Fujiwara, T.; Shirotake, S.; Tomita, K. *Acta Crystallogr.* **1979**, *B35*, 965.

(22) (a) Bagieu-Beucher, M. *Acta Crystallogr.* **1990**, *C46*, 238. (b) Kindberg, B. L.; Amma, E. L. *Acta Crystallogr.* **1975**, *B31*, 1492. (c) Ohki, M.; Takenaka, A.; Shimanouchi, H.; Sasada, Y. *Bull. Chem. Soc. Jpn.* **1975**, *48*, 848.

(23) Beatty, A. M.; Helfrich, B. A.; Hogan, G. A.; Redd, H. A. *Cryst. Growth Des.* **2006**, *6*, 122.

(24) Zhao, X. J.; Zhang, Z. H.; Wang, Y.; Du, M. *Inorg. Chim. Acta* **2007**, *360*, 1921.

(25) (a) Kirschner, S. In *Inorganic Synthesis*; Rochow, E. G., Ed.; McGraw-Hill Book Co.: New York, 1960; Vol. 6. (b) Remy, H. In *Treatise on Inorganic Chemistry*; VCH: Weinheim, Germany, 1956.

(26) *CrysAlis RED*,Version 1.170; Oxford Diffraction: Wroclaw, Poland, 2003.

(27) Altomare, A.; Cascarano, M.; Giacovazzo, C.; Guagliardi, A. *J. Appl. Crystallogr.* **1993**, *26*, 343.

(28) Sheldrick, G. M. *SHELXL97*; Universitat of Göttingen, Germany, 1997.

(29) Farrugia, L. J. *WINGX, A Windows Program for Crystal Structure Analysis*; University of Glasgow: Great Britain, 1998.

(30) Becke, A. D. *J. Chem. Phys.* **1993**, *98*, 5648.

(31) (a) Miehlich, B.; Savin, A.; Stoll, H.; Preuss, H. *Chem. Phys. Lett.* **1989**, *157*, 2000. (b) Lee, C.; Yang, W.; Parr, R. G. *Phys. Rev.* **1988**, *B37*, 785.

(32) Frisch, M. J.; Trucks, G. W.; Schlegel, H. B.; Scuseria, G. E.; Robb, M. A.; Cheeseman, J. R.; Montgomery, Jr., J. A.; Vreven, T.; Kudin, K. N.; Burant, J. C.; Millam, J. M.; Iyengar, S. S.; Tomasi, J.; Barone, V.; Mennucci, B.; Cossi, M.; Scalmani, G.; Rega, N.; Petersson, G. A.; Nakatsuji, H.; Hada, M.; Ehara, M.; Toyota, K.; Fukuda, R.; Hasegawa, J.; Ishida, M.; Nakajima, T.; Honda, Y.; Kitao, O.; Nakai, H.; Klene, M.; Li, X.; Knox, J. E.; Hratchian, H. P.; Cross, J. B.; Bakken, V.; Adamo, C.; Jaramillo, J.; Gomperts, R.; Stratmann, R. E.; Yazyev, O.; Austin, A. J.; Cammi, R.; Pomelli, C.; Ochterski, J. W.; Ayala, P. Y.; Morokuma, K.; Voth, G. A.; Salvador, P.; Dannenberg, J. J.; Zakrzewski, V. G.; Dapprich, S.; Daniels, A. D.; Strain, M. C.; Farkas, O.; Malick, D. K.; Rabuck, A. D.; Raghavachari, K.; Foresman, J. B.; Ortiz, J. V.; Cui, Q.; Baboul, A. G.; Clifford, S.; Cioslowski, J.; Stefanov, B. B.; Liu, G.; Liashenko, A.; Piskorz, P.; Komaromi, I.; Martin, R. L.; Fox, D. J.; Keith, T.; Al-Laham, M. A.; Peng, C. Y.; Nanayakkara, A.; Challacombe, M.; Gill, P. M. W.; Johnson, B.; Chen, W.; Wong, M. W.; Gonzalez, C.; Pople, J. A.; Gaussian, Inc., Wallingford, CT, 2004.

(33) (a) Morozov, A. V.; Kortemme, T.; Tsemekhman, K.; Baker, D. *Proc. Natl. Acad. Sci. U. S. A.* **2004**, *101*, 6946. (b) Sukhanov, O. S.; Shiskin, O. V.; Gorb, L.; Podolyan, Y.; Leszczynskii, J. *J. Phys. Chem. B* **2003**, *107*, 2846. (c) Rappe, A. K.; Bernstein, E. R. *J. Phys. Chem. A* **2000**, *104*, 6117.

(34) (a) Boys, S. F.; Bernardi, F. *Mol. Phys.* **1970**, *19*, 553. (b) Janssen, H. B.; Ross, P. *Chem. Phys. Lett.* **1969**, *3*, 140.

(35) (a) Vaidhyanathan, R.; Natarajan, S.; Rao, C. N. R. *Dalton Trans.* **2001**, 699. (b) Román, P.; Guzmán-Miralles, C.; Luque, A. *Acta Crystallogr.* **1993**, *C49*, 1336.

(36) (a) García-Couceiro, U.; Castillo, O.; Luque, A.; García-Terán, J. P.; Beobide, G.; Román, P. *Cryst. Growth Des.* **2006**, *6*, 1839. (b) García-Couceiro, U.; Castillo, O.; Luque, A.; García-Terán, J. P.; Beobide, G.; Román, P. *Eur. J. Inorg. Chem.* **2005**, 4280.

(37) Kelly, R. E. A.; Kantorovich, L. N. *J. Mater. Chem.* **2006**, *16*, 1894.

(38) Sessler, J. L.; Jayawickramarajah, J. *Chem. Comm.* **2005**, 1939.

(39) Allen, F. H. *Acta Crystallogr.* **2002**, *B58*, 380.

(40) Barker, D. L.; Marsh, R. E. *Acta Crystallogr.* **1964**, *17*, 1581.

(41) Jeffrey, G. A.; Kinoshita, Y. *Acta Crystallogr.* **1963**, *16*, 20.

(42) (a) Armentano, D.; De Munno, G.; Rossi, R. *New J. Chem.* **2006**, *30*, 13. (b) Fujinami, F.; Ogawa, K.; Arakawa, K.; Shirotake, S.; Fujii, S.; Tomita, K. *Acta Crystallogr.* **1979**, *B35*, 968. (c) Tamura, C.; Sato, S.; Hata, T. *Bull. Chem. Soc. Jpn.* **1973**, *46*, 2388. (d) Tamura, C.; Hata, T.; Sato, S.; Sakurai, N. *Bull. Chem. Soc. Jpn.* **1972**, *45*, 3254.

(43) Perumalla, S. R.; Suresh, E.; Pedirredi, V. R. *Angew. Chem., Int. Ed. Engl.* **2005**, *44*, 7752.

(44) (a) Mazurkiewicz, K.; Haranczy, K. M.; Gutowski, M.; Rak, J.; Radisic, D.; Eustis, S. N.; Wang, D.; Bowen, K. H. *J. Am. Chem. Soc.* **2007**, *129*, 1216. (b) Sagstuen, E.; Close, D. M.; Vagane, R.; Hole, E. O.; Nelson, W. H. *J. Phys. Chem. A* **2006**, *110*, 8653.

(45) Teh, A. H.; Kimura, M.; Yamamoto, M.; Tanaka, N.; Yamaguchi, I.; Kumasaka, T. *Biochemistry* **2006**, *45*, 7825.

(46) Kang, C.; Berger, I.; Lockshin, C.; Ratliff, R.; Moyzis, R.; Rich, A. *Proc. Natl. Acad. Sci. U. S. A.* **1995**, *92*, 3874.

(47) (a) Murphy, C. A.; Cameron, T. S.; Cooke, M. W.; Aquino, M. A. S. *Inorg. Chim. Acta* **2000**, *305*, 225. (b) Grey, I. E.; Madsen, I. C.; Sirat, K.; Smith, P. W. *Acta Crystallogr.* **1985**, *C41*, 681.

(48) Hu, G.; Gershon, P. D.; Hodel, A. E.; Quiocho, F. A. *Proc. Natl. Acad. Sci. U. S. A.* **1999**, *96*, 7149.

(49) (a) Perpetuo, G. P.; Janczak, J. *Acta Crystallogr.* **2006**, *C62*, o372. (b) Zhang, X. L.; Chen, X. M. *Cryst. Growth Des.* **2005**, *5*, 617.

(50) Keene, T. D.; Hursthouse, M. B.; Price, D. J. *Z. Anorg. Allg. Chem.* **2004**, *630*, 350.

CG0705916